Journal of Renewable Materials
DOI:10.32604/jrm.2020.08449
Article

Tech Science Press

Ultrasound Assisted Synthesis of Starch Nanocrystals and It's Applications with Polyurethane for Packaging Film

Vikas S. Hakke[1], Uday D. Bagale[1], Sami Boufi[2], G. Uday Bhaskar Babu[1] and Shirish H. Sonawane[1,*]

[1]Department of Chemical Engineering, National Institute of Technology, Warangal (TS), 506004, India
[2]University of Sfax, Sfax Faculty of Science, LMSE, Sfax, Tunisia
*Corresponding Author: Shirish H. Sonawane. Email: shirish@nitw.ac.in
Received: 26 August 2019; Accepted: 20 November 2019

Abstract: Starch nanocrystals (SNC) were prepared from maize starch using ultrasound assisted acid hydrolysis. The process takes less time for the generation of SNC, which is advantageous over conventional acid hydrolysis. The synthesized SNC were characterized using X-ray diffraction, dynamic light scattering, zeta potential and transmission electron microscopy (TEM). Particle size and TEM data show that the particles were near to 150 nm, with oval morphology. The SNC with higher surface charge are obtained with this innovative approach as compared to conventional acid hydrolysis. Because of high surface charge and oval like morphology, the SNC performed well in reinforcing a polyurethane film. The rise in crystallinity by 16% was observed due to ultrasound cavitation. At the lower concentration of SNC in nanocomposite film, dynamic mechanical analysis demonstrated meaningful increment in mechanical properties of polyurethane nanocomposite film. The decrease in chain slippage over the glass transition temperature was observed because of the SNC reinforcement in polyurethane dispersion. Compared to the conventional acid hydrolysis, the present approach for the synthesis of starch nanocrystals is much faster and easier.

Keywords: Starch; nanocrystal; ultrasound; acid-hydrolysis; nanocomposite; TEM

1 Introduction

Over the years, nanomaterials such as cellulose, chitin and starch have gained an increasing attention due to their heteropolymeric structure, sustainability, green and environment friendly nature for various applications [1-3]. The nanosize materials have a greater impact on their physical properties such as rise in surface to volume ratio. The nanoparticles with high surface to volume ratio are utilized as reinforcement materials, as they show good binding capacity, and mechanical properties. The blending of nanoparticles reduces the density of synthesized material [4,5]. Due to these novel characteristics of nanocrystals, the synthesis approaches and utilization of starch nanocrystals (SNC) have been reviewed extensively. It has been found that, the acid hydrolysis is the simplest method for the synthesis of SNC [6-8].

The onion like structure of starch consists of amorphous and crystalline planes alternatively, which makes it difficult to convert it into a 100% crystalline structure. Acid with high concentration was employed in

conversion of amorphous part of the starch in conventional SNC synthesis process. However, there is an issue regarding the processing time and lower yields (below 10%) [9-11]. The number of attempts have been made in order to improve the yield and lower down the processing time [11,12]. Recently, the application of the sonochemical approach for breaking the aggregates of starch particles to form nanoparticles has been reported. Kim et al. [13] reported, the formation of waxy starch nanoparticles from rice grains using the sonochemical approach in the presence of ethanol. They also reported the effect of sonication on the particle size. They found that sonication increases the rate of SNC generation but at the cost of crystallinity. Kim et al. [14] in another study reported the synthesis of SNC using waxy maize starch by the combined effect of hydrolysis and ultrasound at a lower temperature of 4°C in which the crystallinity of starch was slightly increased. Haaj et al. [15] explained the synthesis of starch nanoparticles from normal and waxy starch by using ultrasound. They found that, the synthesized nanoparticles were amorphous in nature.

The synthesis of SNC via ultrasound assisted acid hydrolysis of starch was inspired by the synthesis of cellulose nanofibres from cellulose. As many researches are working on ultrasound-assisted synthesis of nanofibers from cellulosic sources [16-19] and evaluated the effects of temperature, concentration, power, size, time and distance from probe tip to beaker on the degree of fibrillation of cellulose. They reported that better fibrillation was caused by higher power sonication at elevated temperature. However, higher concentration and larger distance from probe to beaker were not advantageous for fibrillation. The yield of nanocellulose production was 71% due to cavitating bubbles formed in the presence of ultrasound when ultrasound-TEMPO oxidizing method was used [20]. They summarized that mechanical treatment by blender (90% yield in 40 min) and ultrasound probe (100% yield in 25 min) with high ultrasonication intensity was more efficient for the production of nanocellulose in contrast to bath sonication (50% yield in 60 min). They also suggested that the ultrasound technique is useful for the degradation of materials like cellulose and starch for the synthesis of nanophase.

Polyurethane is a widely used polymer in film casting and coating industries. The growth of polyurethane is highly dependent on the availability of cheap feedstocks such as poly-isocyanates, polyols, and chain extender with co-reactants such as water, alcohols, and amines. In principle, there is as much potential for design of isocyanate structures as there is for alcohol and amine co-reactants. Utilization of starch nanoparticles as nanofillers, synthesis of novel starch based nanocomposite films and their applications has been widely studied in recent past [21-24]. Balakrishnan et al. [25] synthesized potato starch-based biocomposite film, which is UV resistant in nature and helps to alter the shelf life of the food material. The addition of nanofillers of cellulose in the potato starch film helps to improve the barrier and mechanical properties of nanocomposite film with lower loading ratio.

The present work highlights a rapid synthesis of SNC. Synthesized SNC are utilized as nanofiller in polyurethane to produce nanocomposite films. Ultrasound assisted acid hydrolysis method has been employed for the production of SNC. The article deals with the study of addition of SNC in polyurethane complex. Nanocomposite films are prepared and studied for the mechanical properties and solubility. New generation of nanocomposite films can be a good option for the packaging films. The present work significantly opens a path for the application of SNC as nanofiller in the polyurethane matrix. The effect of SNC on polyurethane dispersion with respect to DMA analysis has been studied. The presented nanocomposite film may act as a packaging film for the food system.

2 Materials and Methods

2.1 Materials

Maize corn starch (27.5 ± 1.2% amylose content), sulphuric acid and polyurethane resin were purchased from Alfa aesar and Merck respectively. Vacuum filtration was used for the filtration of hydrolyzed starch. In all the preparations, deionized (D. I.) water was used.

2.2 Starch Nanocrystals Preparation

Ultrasound assisted acid hydrolysis was adopted for the synthesis of SNC as follows; 1.67 g of starch was mixed in D. I. water (55 mL) and sonicated for 20 min using 20 kHz probe sonicator (Dakshin ultrasonicator, Mumbai, India) of tip size 20 mm at the power input of 220 watts (3 sec on and 1 sec off, pulse mode). In the presence of ultrasonic irradiation, 0.25 M (50 mL) sulphuric acid was added dropwise in the above starch-water solution for the next 20 min. In order to achieve maximum acid hydrolysis sonication was continued for another 30 min at 30°C. 0.25 M (50 mL) NaOH solution was used to neutralize the unreacted acid, the dropwise addition proceeds until a pH of 7 was achieved at room temperature. The above solution was then subjected to centrifugation at 9000 rpm for 20 min followed by washing with 600 mL D. I. water in order to remove the impurities like traces of acid and base. The thick slurry was then dried in a desiccator and powder form of SNC were produced. Thereby ultrasound-assisted acid hydrolyzed SNC was obtained.

For the comparison, SNC was also synthesized by conventional acid hydrolysis. Sulphuric acid (0.2 M) was utilized for the acid hydrolysis of native starch and kept under magnetic stirring for 48 h, followed by neutralization, centrifuge and drying as mentioned above.

2.3 Film Preparation

0.04 g of SNC was blended with 2 g of polyurethane (0.32 g solid/mL of dispersion) aqueous dispersion in 10 mL D. I. water. Sonication was used for the uniform blending of SNC in polyurethane dispersion. A film was prepared by casting methodology in a glass petri dish and stored in the desiccator until characterizations were performed.

2.4 Analysis

2.4.1 Particle Size Analysis and Zeta Potential Measurement

Particle size and zeta potential measurements of SNC were performed at 25°C using a Malvern nanosizer (Nano ZS, ZEN 3600) using dynamic light scattering (DLS) method. SNC was added in D. I. water and homogenized by using bath sonication until an obscuration of less than 10% was recorded. A value of 1.33 was used as a refractive index and the particle size distribution of samples was characterized based on a DLS method.

2.4.2 Microstructure Characterization

Transmission electron microscopy (TEM, PHILIPS, CM 200) operated at 200 Kv with resolution 2.4 A° was used to observe the surface morphology of the fabricated nanocrystals. A drop of nanocrystal suspension (0.2% w/v) was spread on a glow discharged carbon-coated TEM grid.

2.4.3 Thermogravimetric Analysis (TGA) of SNC

TGA analysis was done with TGA-6/DTG of NETZSCH STA 2500 (precision of temperature measurement ± 2°C, microbalance sensitivity < 5 μg). The percentage weight loss of the sample was recorded continuously as function of temperature, under dynamic conditions, in the range of 30-600°C. The experiments were carried out at atmospheric pressure, under a nitrogen atmosphere, with a flow rate of 60 mL/min, at a linear heating rate of 10°C/min. The small mass of sample material i.e., 20 mg was filled in the crucible whereas the reference crucible was kept empty in case of native starch as well as SNC. The experiment was carried out in triplicate to check the reproducibility of results.

2.4.4 X-ray Diffraction (XRD) Analysis

Bruker D8 advanced X-ray diffractometer was used to collect the XRD spectra of the SNC and nanocomposite films. Copper Kα (Cu Kα) radiations were used to produce the X-rays with the

wavelength of 0.154 nm and were recorded on the 2θ scale, ranging from 5° to 50° with the step size of 0.018 in 2θ.

2.4.5 Dynamic Mechanical Analysis (DMA) of the Nanocomposite Film

DMA analysis was used to study the thermo-mechanical properties of nanocomposite films. DMA analyzer was used in tension mode for the film analysis. Pure polyurethane film was compared with the synthesized nanocomposite film of starch and polyurethane to understand the thermo-mechanical properties of the nanocomposite film. The film sample was analyzed under cyclic load with a frequency of 1 Hz and, temperature variation ranging from −50°C to 150°C. The temperature variation rate was kept at 2°C/min. The standard procedure was followed for the calibration of DMA analyzer. The sample of size 20 mm × 5 mm with a thickness of 5 mm was used for the analysis with 20 μm tension in a longitudinal direction. A cooling system with liquid nitrogen was used to cool the sample.

2.4.6 Water Solubility of the Nanocomposite Film

The water solubility of the completely dried nanocomposite film was measured over 24 h. The nanocomposite film was completely dried in a desiccator at room temperature. The weight of dry film was noted as initial weight and then the film was kept in D. I. water for 24 h in the controlled environment. The wet film was then carefully dried and stored in desiccator. The difference between the initial weight and the final weight of dry film will give the weight loss of film in D. I. water during 24 h. The percentage solubility of the film was measured as per Eq. (1).

$$\% \text{ Solubility} = \frac{(\text{initial dry wt. of film} - \text{final dry wt. of film})}{(\text{initial dry wt. of film})} \times 100 \quad (1)$$

Na_2SO_4 ensured complete drying of the film in a desiccator.

3 Results and Discussion

3.1 Particle Size

The particle size of synthesized SNC was ensured with DLS. A very dilute aqueous suspension of dried SNC was sonicated by using bath sonicator for 5 min as mentioned in the standard procedure for the sample preparation. Fig. 1 shows the monomodal nature of recorded scattered light from DLS. The hydrodynamic radius for the starch particles was centred about 200 nm. The particle size of synthesized SNC cannot be confirmed with the DLS alone as it gives overall hydrodynamic sphere radius rather than exact radius for the particle. The synthesis of SNC by the present approach takes very less time as compared to the conventional hydrolysis method. To avoid the effect of acid concentration on the crystallinity of synthesized SNC, low concentration of acid was used in the present method. For the starch nanoparticles synthesized by conventional method of acid hydrolysis, the particle size is reported in Tab. 1. The ultrasound assistance of 50 min and 1 h stirring for synthesis of SNC gives over view on time reduction.

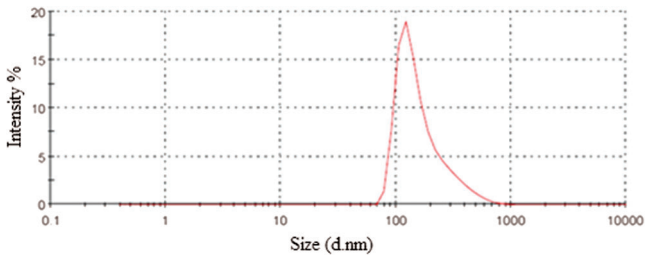

Figure 1: Particle size analysis for SNC

Table 1: Average particle size and zeta potential measurement of SNC by DLS

Sr. No.	Sample Name	Average Size (nm)	Average Zeta Potential (mV)
1	SNC Ultrasound assisted Hydrolysis	253	−21.6
2	SNC Conventional Hydrolysis	2581	−6.98

The yield of SNC was found to be 36% by mass balance method. The combined effect reduces the time interval as well as more efficiently increases the yield. Amini et al. [26] have reported that the starch particles may not be fully hydrolyzed. They reported that a lower concentration of acid would give rise to the nanoscale particle size of starch; the yield is more at a higher temperature and with more sonication time. Degradation yield of starch granules at higher temperature was observed to be equivalent to the present yield [14].

3.2 Zeta Potential

Surface charge on the SNC synthesized by conventional and ultrasound assisted hydrolysis methods was found and reported in Tab. 1. It was found that, the zeta potential of SNC synthesized by conventional method has lower value than that of SNC synthesized by ultrasound assisted acid hydrolysis method. A lower value of zeta potential indicates unstable suspension. Negative value of both SNC indicates the presence of sulphate group ($-OSO_3^-$) on the surface of SNC. It has also been reported that the presence of sulphate group ($-OSO_3^-$) on the surface of SNC was responsible for negative zeta potential value [27]. SNC synthesized by hydrolysis has much higher stability as compared to other methods of synthesis such as TEMPO oxidation [10] or ultrasound [15] because of the presence of negative charge, presence of electrostatic repulsion between similarly charged SNC did not allow them to agglomerate. Zeta potential of SNC was found to be enhanced with ultrasound assistance.

3.3 Morphology Study of Starch Nanocrystals

Fig. 2 represents the TEM image of synthesized SNC. From Fig. 2, it is observed that, SNC with oval shape morphology and size in the range of 15-150 nm was obtained, which is in harmony with DLS measurement. Kim et al. [13] reported the different methods for the synthesis of SNC including the three-stage effective hydrolysis. They also mentioned that acid hydrolysis is a slow process with the starch as it has a semi-crystalline structure.

The speed of acid hydrolysis depends upon the packaging structure of crystalline regime of starch and total crystallinity of starch. Boufi et al. [27] and Shabana et al. [28] reported different shapes of SNC such as

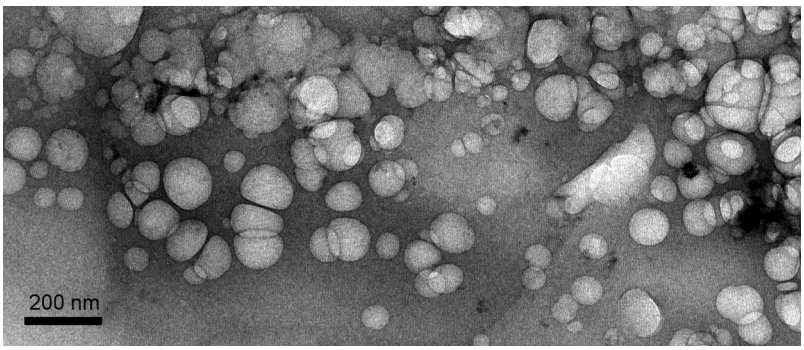

Figure 2: TEM image of SNC

round edge, polygon and irregular platelets this is due to the extent of hydrolysis completed with starch granules. The synthesis of SNC with combined effect of sonication and acid hydrolysis was confirmed with the TEM image.

3.4 Crystallinity Comparison of SNC Synthesized by Conventional Hydrolysis and Ultrasound Assisted Hydrolysis

It was observed from the XRD pattern of SNC in Fig. 3, that the highest peak exists at 2θ value of 17.90°, and its full width at half maximum intensity of the peak is 0.5668, for the X-ray wavelength of 0.1540 nm. The Debye-Scherer formula provides the average crystallite size of 14.83 nm, which is analogous to TEM analysis.

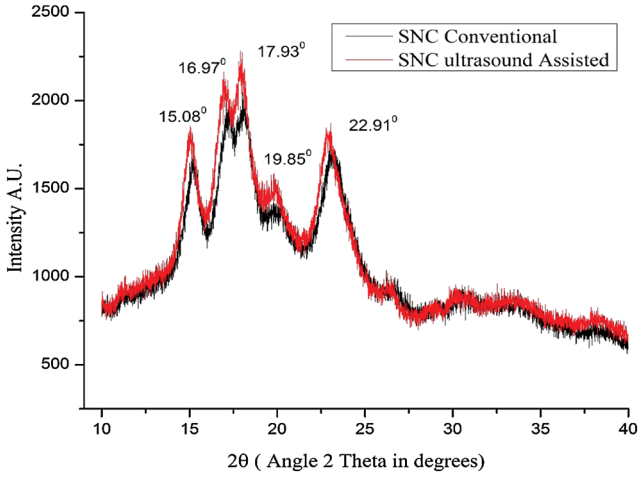

Figure 3: XRD analysis of SNC synthesized by both methods

Crystallinity is an important characteristic of the nanostructure. Polysaccharide starch is made up of glucose. The amylose and amylopectin are major parts of starch due to which it is identified as natural polymer. Amorphous regions of starch granules are attributed to the presence of amylose whereas amylopectin represents the crystalline region of the starch. The high frequency of sonication breaks the starch granules in smaller parts due to which amorphous region of granule interact with the acid and speed of hydrolysis is enhanced. The similar mechanism was reported by Baufi et al. [29].

The combined effect of ultrasonication and acid hydrolysis eliminates the amorphous region of native starch to some extent. Fig. 3 shows comparison of SNC synthesized by two different approaches. Fig. 3 shows the comparison of native SNC synthesized with conventional acid hydrolysis as well as by ultrasound assisted acid hydrolysis. The increase in the crystallinity index of SNC synthesized by ultrasound assisted acid hydrolysis was observed to be 21.6% as compared to SNC synthesized by conventional acid hydrolysis. The area under the sharp peaks observed for the SNC synthesized by ultrasound assisted acid hydrolysis was higher than the area under the sharp peaks for the SNC synthesized by conventional acid hydrolysis. This rise in the area under the sharp peaks indicates significant increase in the crystallinity of SNC synthesized by ultrasound assisted acid hydrolysis. The rise in crystallinity by 16% was observed due to ultrasound assistance. The XRD pattern reported by Amini et al. [26] shows lower crystallinity effect as compared to the presented method for the synthesis of SNC. They prepared the SNC with an acid concentration of 4.5 M that is very high in comparison with the present work of acid concentration of 0.25 M. This indicates that there is a significant effect of

sonication on the crystallinity of SNC. Many researchers have reported that the higher time of sonication and temperature may lead to a decrease in crystallinity of SNC [10-11]. On the contrary, to this, we did not notice any decrease in crystallinity, presumable due to the contribution of ultrasound in reducing the time for the hydrolysis process. In addition to this, the rise in crystallinity of SNC synthesized with acid hydrolysis was successfully reported [13-15].

In Fig. 4 the X-ray diffraction pattern of SNC, PU film, and nanocomposite film composed of PU and SNC is shown. The X-ray diffraction pattern of SNC shows sharp peaks in between 15° to 25° indicating crystalline nature of synthesized SNC. However, when SNC is blended with PU matrix to produce nanocomposite film, the amorphous nature of PU dominates the crystalline nature of SNC.

The comparative study of crystallinity of PU film and SNC-PU nanocomposite film is also represented in Fig. 4. It shows that, on the addition of synthesized SNC to the PU matrix to prepare PU-SNC nanocomposite film, significant reduction in area under the broad peak in between 10° to 40° diffraction angle is observed. This reduction in area clearly indicates that, addition of SNC in PU matrix increases the crystallinity of synthesized PU-SNC nanocomposite film as compared to plain PU film. The increase in crystallinity of PU-SNC nanocomposite film is found to be 46%. In nanocomposite film, the diffraction peaks of SNC were no longer visible, presumably due to the low content of SNC in PU matrix.

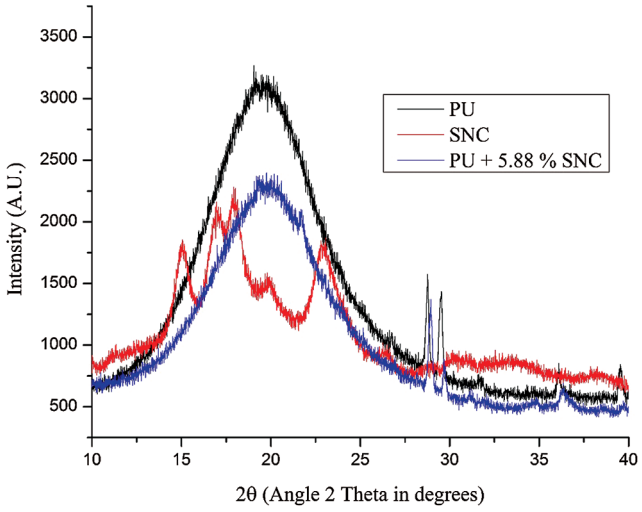

Figure 4: XRD analysis of crystallinity of Plain PU film, SNC powder, and PU + 5.88% SNC Nanocomposite film

3.5 Thermal Properties of SNC

The TGA analysis of SNC produced by both conventional and hybrid methodology is shown in Fig. 5. The SNC produced by both methods, first showed a weight loss around 120°C due to the evaporation of moisture content in the sample, where water bonds with starch get break. In the second stage a sudden weight loss, around 300°C was observed with different rates in both SNC. The SNC synthesized with conventional hydrolysis method has sharp drop due to presence of higher amorphous portion in SNC, while in other the weight loss increases gradually. The result ensures the rise in extent of hydrolysis of starch and crystallinity of SNC. The results are in resemblance with as reported by Namazi et al. [30], Castano et al. [31] and Varma et al. [32].

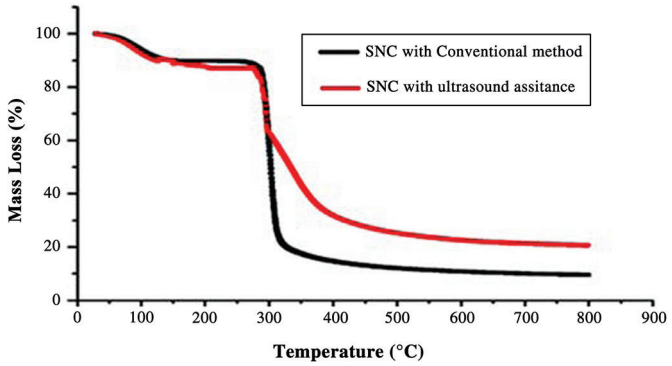

Figure 5: TGA analysis for SNC synthesized by both methods

3.6 Effect of SNC Reinforcement in Polyurethane Matrix

To investigate the reinforcing potential of SNC, nanocomposite films have been prepared by film casting of a mixture of SNC suspension and a commercial polyurethane dispersion (PUD). The resulting translucid films were analyzed by DMA over a wide domain of temperature from the glassy to the elastic domain over the glass transition. DMA was used to understand the intermolecular interaction between SNC and polyurethane. The evaluation of the storage modulus (E′) *vs*. the temperature at the different composition of nanocomposite films is shown in Fig. 6.

The pure polyurethane (PU) matrix remained hard in a glassy state till −25°C with storage modulus E' around 1 GPa. A 2.5-decade drop in E′ over more than 70°C domain of temperature is observed associated with the glass transition of the amorphous part of the PU matrix. This transition is accompanied by a maximum in tan δ around 20°C. At 75°C, an abrupt and steep fall of E' is observed which is presumably associated with the melting of the crystalline fraction of the PU and the chain slippage under the effect of increased mobility. Chen et al. [33] had reported similar results. They studied the PU-SNC nanocomposite matrix with different temperature range as from −150°C to 100°C, they found that at high temperature interaction between molecules is weaker which is the reason for increasing mobility.

The inclusion of SNC led to a meaningful enhancement of the modulus over the glass transition without affecting the stiffness in glass domain. At 50°C, the increment in E' was about 3.5, 7 and 27 at an SNC content of 5%, 10% and 30% respectively. However, this reinforcing effect is lower compared to cellulose-based nanocomposites. Another effect brought by the inclusion of SNC on the PU matrix is the prevention of macromolecular chain slippage over glass transition as attested by a shift of the fall of E' above the T_g and its full vanishing as the content of SNC exceeded 5%. This effect can be explained by the formation of some interconnected network involving SNC and the polymer phase, restraining the mobility and flow of the polymer chains. Over the percolation threshold, the interconnected SNC network was held through strong hydrogen bonding contributed to further restrains, and the long-range motion preventing them from slippage and flowing.

3.7 Water Solubility of the Starch Based Polyurethane Composite Films

Water solubility is an important factor to be considered for packaging materials. The solubility of the film affects the efficiency of packaging, it also effects on the environment of storage condition when packaging material is applied. In some cases, solubility may be helpful as in the case of un-ripening of food material if the solubility of packaging is high it can be easily removed with the help of water. Addition of SNC in PU dispersion will decrease the solubility of film. Fig. 7 gives clarification on the observed values for the 24 h at room temperature. PU film and nanocomposite film was compared for

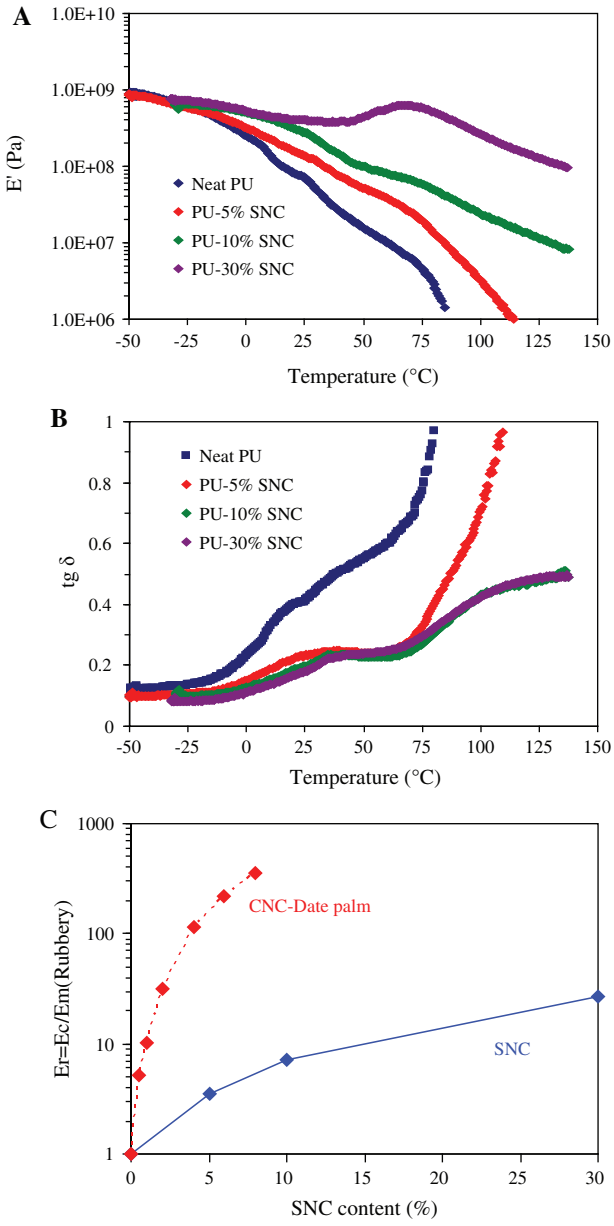

Figure 6: DMA analysis of nanocomposite films: (A) storage modulus E as function of temperature, (B) Loss factor (tan δ) plotted as function of Temperature, and (C) Storage modulus *vs.* composition of nanocomposite film at 50°C

random three samples and average percentage solubility was calculated. The final weight of the films was noted after the complete removal of moisture. It was observed that the solubility of PU film was decreased from 2% to 1.6% due to the addition of SNC nanofillers. SNC interaction of PU makes the structure more floppy and impermeable to water by strong hydrogen bonds with −NH group of PU matrix. The concentration of SNC may also affect the permeability of water across the film, which is not reported yet.

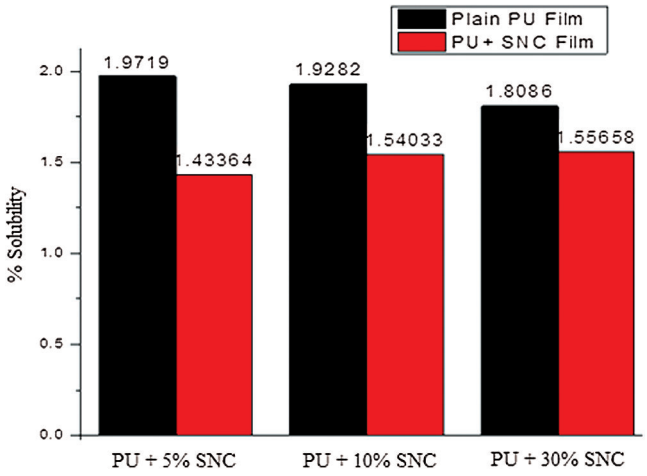

Figure 7: Water solubility for PU film and PU + SNC film for 24 h

4 Conclusion

The hybrid technology proposed in this work has demonstrated successful synthesis of SNC. The oval platelet-shaped SNC were synthesized with improved efficiency in less time. The yield of 36% was obtained for the synthesized SNC with low concentration of acid. Remarkable reduction in time was also observed that is from 48 h in conventional hydrolysis process to 2 h in proposed ultrasound assisted hydrolysis process, as the ultrasound irradiation enhances the rate of acid hydrolysis of starch. The average particle size of 50-100 nm was obtained for 45-50 min sonication time. The significant effect of sonication on the crystallinity of SNC was ensured with the comparative study of XRD. The rise in crystallinity by 16% was observed due to ultrasound assistance. A crystallinity index of 21.6% was found for SNC synthesized by ultrasound assisted acid hydrolysis. The synthesized SNC was blended with a PU matrix to obtain the nanocomposite film. The decrease in solubility of nanocomposite film from 2% to 1.6% was noticed in the aqueous phase. The SNC-PU nanocomposite film demonstrated better mechanical properties and lower water solubility as compared to a pure PU film.

Acknowledgment: Authors acknowledge to Ministry of Science and Technology India, Department of Science and Technology international bilateral cooperation division, for financial assistance through Indo Tunisia Project grant no DST/INT/TUNISIA/P-06/2017.

Funding Statement: The author(s) received no specific funding for this study.

Conflicts of Interest: The authors declare that they have no conflicts of interest to report regarding the present study.

References

1. Kim, H. Y., Han, J. A., Kweon, D. K., Park, J. D., Lim, S. T. (2013). Effect of ultrasonic treatments on nanoparticle preparation of acid-hydrolyzed waxy maize starch. *Carbohydrate Polymers, 93(2),* 582–588. DOI 10.1016/j.carbpol.2012.12.050.
2. Alcazar-Alay, S. C., Meireles, M. A. A. (2015). Physicochemical properties, modifications and applications of starches from different botanical sources. *Food Science and Technology, 35(2),* 215–236. DOI 10.1590/1678-457X.6749.

3. Dufresne, A. (2014). Crystalline starch based nanoparticles. *Current Opinion in Colloid & Interface Science, 19 (5),* 397–408. DOI 10.1016/j.cocis.2014.06.001.
4. Hu, F., Fu, S., Huang, J., Anderson, D. P., Chang, P. R. (2015). Structure and properties of polysaccharide nanocrystals. In: Huang, J., Chang, P. R., Lin, N., Dufresne, A., (eds.) *Polysaccharide-based Nanocrystals: Chemistry and Applications*. Weinheim: Wiley-VCH Verlag GmbH & Co. KGaA, 15–62.
5. Kim, H. Y., Park, S. S., Lim, S. T. (2015). Preparation, characterization and utilization of starch nanoparticles. *Colloids and Surfaces B: Biointerfaces, 126,* 607–620. DOI 10.1016/j.colsurfb.2014.11.011.
6. Khalil, H. A., Davoudpour, Y., Islam, M. N., Mustapha, A., Sudesh, K. et al. (2014). Production and modification of nanofibrillated cellulose using various mechanical processes: a review. *Carbohydrate Polymers, 99,* 649–665. DOI 10.1016/j.carbpol.2013.08.069.
7. Le Corre, D., Angellier-Coussy, H. (2014). Preparation and application of starch nanoparticles for nanocomposites: a review. *Reactive and Functional Polymers, 85,* 97–120. DOI 10.1016/j.reactfunctpolym.2014.09.020.
8. Lin, N., Huang, J., Chang, P. R., Anderson, D. P., Yu, J. (2011). Preparation, modification, and application of starch nanocrystals in nanomaterials: a review. *Journal of Nanomaterials, 2011,* 20. DOI 10.1155/2011/573687.
9. Lin, N., Huang, J., Chang, P. R., Anderson, D. P., Yu, J. (2011). Preparation, modification, and application of starch nanocrystals in nanomaterials: a review. *Journal of Nanomaterials, 2011,* 1–13.
10. Le Corre, D., Bras, J., Dufresne, A. (2010). Starch nanoparticles: a review. *Biomacromolecules, 11(5),* 1139–1153. DOI 10.1021/bm901428y.
11. Kim, H. Y., Park, S. S., Lim, S. T. (2015). Preparation, characterization, and utilization of starch nanoparticles. *Colloids and Surfaces B: Biointerfaces, 126,* 607–620. DOI 10.1016/j.colsurfb.2014.11.011.
12. Mary, S. K., Pothan, L. A., Thomas, S. (2013). Applications of starch nanoparticles and starch-based bionanocomposites. In: Dufresne, A., Thomas, S., Pothen, L. A., (eds.) *Biopolymer Nanocomposites: Processing, Properties, and Applications*. New Jersey: John Wiley & Sons Inc, 293–307.
13. Kim, H. Y., Park, D. J., Kim, J. Y., Lim, S. T. (2013). Preparation of crystalline starch nanoparticles using cold acid hydrolysis and ultrasonication. *Carbohydrate Polymers, 98(1),* 295–301. DOI 10.1016/j.carbpol.2013.05.085.
14. Kim, H. Y., Han, J. A., Kweon, D. K., Park, J. D., Lim, S. T. (2013). Effect of ultrasonic treatments on nanoparticle preparation of acid-hydrolyzed waxy maize starch. *Carbohydrate Polymers, 93(2),* 582–588. DOI 10.1016/j.carbpol.2012.12.050.
15. Haaj, S. B., Magnin, A., Pétrier, C., Boufi, S. (2013). Starch nanoparticles formation via high power ultrasonication. *Carbohydrate Polymers, 92(2),* 1625–1632. DOI 10.1016/j.carbpol.2012.11.022.
16. Cheng, Q., Wang, S., Rials, T. G. (2009). Poly (vinyl alcohol) nanocomposites reinforced with cellulose fibrils isolated by high intensity ultrasonication. *Composites Part A: Applied Science and Manufacturing, 40(2),* 218–224. DOI 10.1016/j.compositesa.2008.11.009.
17. Frone, A. N., Panaitescu, D. M., Donescu, D., Spataru, C. I., Radovici, C. et al. (2011). Preparation and characterization of PVA composites with cellulose nanofibers obtained by ultrasonication. *BioResources, 6(1),* 487–512.
18. Wang, H., Li, D., Zhang, R. (2013). Preparation of ultralong cellulose nanofibers and optically transparent nanopapers derived from waste corrugated paper pulp. *BioResources, 8(1),* 1374–1384.
19. Tang, Y., Yang, S., Zhang, N., Zhang, J. (2014). Preparation and characterization of nanocrystalline cellulose via low-intensity ultrasonic-assisted sulfuric acid hydrolysis. *Cellulose, 21(1),* 335–346. DOI 10.1007/s10570-013-0158-2.
20. Mishra, S. P., Manent, A. S., Chabot, B., Daneault, C. (2012). Production of nanocellulose from native cellulose-various options utilizing ultrasound. *BioResources, 7(1),* 422–436.
21. Slavutsky, A. M., Bertuzzi, M. A., Armada, M. (2012). Water barrier properties of starch-clay nanocomposite films. *Brazilian Journal of Food Technology, 15(3),* 208–218. DOI 10.1590/S1981-67232012005000014.
22. Zia, F., Zia, K. M., Zuber, M., Kamal, S., Aslam, N. (2015). Starch based polyurethanes: a critical review updating recent literature. *Carbohydrate Polymers, 134,* 784–798. DOI 10.1016/j.carbpol.2015.08.034.

23. Babu, R. P., Oconnor, K., Seeram, R. (2013). Current progress on bio-based polymers and their future trends. *Progress in Biomaterials, 2(1),* 8. DOI 10.1186/2194-0517-2-8.
24. Elsabee, M. Z., Abdou, E. S. (2013). Chitosan based edible films and coatings: a review. *Materials Science and Engineering: C, 33(4),* 1819–1841. DOI 10.1016/j.msec.2013.01.010.
25. Balakrishnan, P., Gopi, S., Thomas, S. (2018). UV resistant transparent bionanocomposite films based on potato starch/cellulose for sustainable packaging. *Starch-Stärke, 70(1-2),* 1700139. DOI 10.1002/star.201700139.
26. Amini, A. M., Razavi, S. M. A. (2016). A fast and efficient approach to prepare starch nanocrystals from normal corn starch. *Food Hydrocolloids, 57,* 132–138. DOI 10.1016/j.foodhyd.2016.01.022.
27. Boufi, S., Haaj, S. B., Magnin, A., Pignon, F., Imperor-Clerc, M. et al. (2018). Ultrasonic assisted production of starch nanoparticles: structural characterization and mechanism of disintegration. *Ultrasonics Sonochemistry, 41,* 327–336. DOI 10.1016/j.ultsonch.2017.09.033.
28. Shabana, S., Prasansha, R., Kalinina, I., Potoroko, I., Bagale, U. et al. (2019). Ultrasound assisted acid hydrolyzed structure modification and loading of antioxidants on potato starch nanoparticles. *Ultrasonics Sonochemistry, 51,* 444–450. DOI 10.1016/j.ultsonch.2018.07.023.
29. Boufi, S., Kaddami, H., Dufresne, A. (2014). Mechanical performance and transparency of nanocellulose reinforced polymer nanocomposites. *Macromolecular Materials and Engineering, 299(5),* 560–568. DOI 10.1002/mame.201300232.
30. Namazi, H., Dadkhah, A. (2010). Convenient method for preparation of hydrophobically modified starch nanocrystals with using fatty acids. *Carbohydrate Polymers, 79(3),* 731–737. DOI 10.1016/j.carbpol.2009.09.033.
31. Castano, J., Bouza, R., Rodriguez-Llamazares, S., Carrasco, C., Vinicius, R. V. B. (2012). Processing and characterization of starch-based materials from pehuen seeds (Araucaria araucana (Mol) K. Koch). *Carbohydrate Polymers, 88(1),* 299–307. DOI 10.1016/j.carbpol.2011.12.008.
32. Varma, C. A. K., Panpalia, S. G., Kumar, K. J. (2014). Physicochemical and release kinetics of natural and retrograded starch of Indian palmyrah shoots. *International Journal of Biological Macromolecules, 66,* 33–39. DOI 10.1016/j.ijbiomac.2014.02.018.
33. Chen, G., Wei, M., Chen, J., Huang, J., Dufresne, A. et al. (2008). Simultaneous reinforcing and toughening: new nanocomposites of waterborne polyurethane filled with low loading level of starch nanocrystals. *Polymer, 49(7),* 1860–1870. DOI 10.1016/j.polymer.2008.02.020.